

${}^7\text{Li}$ and ${}^{31}\text{P}$ NMR studies of monoclinic $\text{Li}_3\text{In}_2(\text{PO}_4)_3$

I. S. Pronin and A. A. Vashman

All-Russian Institute of Inorganic Materials, ul. Rogova 5, Moscow 123060, Russia

S. E. Sigaryov*

Institute of Crystallography, Russian Academy of Sciences, Leninsky pr. 59, Moscow 117333, Russia

(Received 4 January 1993; revised manuscript received 11 May 1993)

Fourier-transform NMR spectra and spin-lattice relaxation rates were studied for ${}^7\text{Li}$ and ${}^{31}\text{P}$ in a monoclinic modification of the $\text{Li}_3\text{In}_2(\text{PO}_4)_3$ superionic conductor over a wide temperature range of 240–575 K. The static magnetic susceptibility of the lithium subsystem of the compound and the ${}^{31}\text{P}$ NMR line shape exhibit anomalous changes with increasing temperature. Quadrupole structure of the ${}^7\text{Li}$ NMR spectrum is observed under fast motion of the lithium ions in the superionic phase. In this phase the temperature behavior of the spin-lattice relaxation rates is different for ${}^7\text{Li}$ and ${}^{31}\text{P}$ nuclei. The results are discussed taking into account the preceding NMR data on monoclinic $\text{Li}_3\text{Sc}_2(\text{PO}_4)_3$ and rhombohedral $\text{Li}_3\text{In}_2(\text{PO}_4)_3$ compounds.

I. INTRODUCTION

The lithium-indium [$\text{Li}_3\text{In}_2(\text{PO}_4)_3$] and lithium-scandium [$\text{Li}_3\text{Sc}_2(\text{PO}_4)_3$] phosphates are superionic conductors.^{1,2} The superionic state in these compounds appears as a result of phase transitions occurring as the temperature increases. That is why it is of interest to study, with NMR, the effects of both temperature rise and phase transformations on the dynamics of lithium nuclei and their interactions with other nuclei. The data can be compared with the results obtained with other techniques.

Such investigations have been performed earlier with rhombohedral $\text{Li}_3\text{In}_2(\text{PO}_4)_3$ (Ref. 3) and monoclinic $\text{Li}_3\text{Sc}_2(\text{PO}_4)_3$.⁴ These crystals are distinguished by their relaxation rates and NMR spectra as well as values of ionic conductivity and temperatures of superionic phase transitions. These facts can be connected not only with the difference between the chemical formulas of these compounds (In or Sc) but also between their crystal structures.

This paper presents data from investigations of the NMR spectra and spin-lattice relaxation rates for ${}^7\text{Li}$ and ${}^{31}\text{P}$ in a polycrystalline sample of monoclinic $\text{Li}_3\text{In}_2(\text{PO}_4)_3$ isostructural to monoclinic $\text{Li}_3\text{Sc}_2(\text{PO}_4)_3$.⁵ The data are compared with the results obtained for both monoclinic $\text{Li}_3\text{Sc}_2(\text{PO}_4)_3$ and rhombohedral $\text{Li}_3\text{In}_2(\text{PO}_4)_3$. It is noteworthy that the terms “monoclinic” or “rhombohedral” belong only to the room-temperature modifications of these crystals.

The experimental techniques and conditions have been detailed elsewhere.^{3,4}

II. EXPERIMENTAL RESULTS**A. ${}^7\text{Li}$ NMR spectra**

Figure 1 shows the ${}^7\text{Li}$ Fourier-transformed (FT) NMR spectra of monoclinic $\text{Li}_3\text{In}_2(\text{PO}_4)_3$ at different temperatures.

In the low-temperature range (≤ 300 K), the spectrum consists of a superposition of the broad (*A*) and narrow (*B*) components with the same value of the chemical shift. The integral intensities of the components are about of 80% and 20%, respectively, of the total intensity of the NMR spectrum.

With increasing temperature from 300 to 340 K, the intensity of the *A* component reduces almost to zero. The disappearance of the component *A* initially occurs due to the decrease of its amplitude only and then due to the decrease of its extension as well [see Fig. 1(a)].

A new component (*C*) appears in the ${}^7\text{Li}$ NMR spectrum above 340 K. The intensity of the component increases quickly with increasing temperature. At 370 K the component *C* transforms to a well-resolved quadrupole triplet characteristic of a spin of $\frac{3}{2}$ [see Fig. 1(b)]. This triplet has the quadrupole coupling constant $e^2qQ/h = 26.4$ kHz and the value of the asymmetry parameter $\eta = 0.31$.

A second triplet (*D*) with $e^2qQ/h = 9.4$ kHz and $\eta \approx 1.0$ appears abruptly on the background of the *C* triplet at 375 K. The *C* and *D* quadrupole triplets are simultaneously observed in the ${}^7\text{Li}$ spectrum within a narrow temperature range in the vicinity of 375 K. At 380 K the *C* triplet completely disappears and only the *D* triplet remains in the spectrum [see Fig. 1(c)]. The temperature interval corresponding to the *C* ↔ *D* transformation is about 5 K.

The parameters of the *D* triplet vary as the temperature increases in the range 380–575 K. The asymmetry parameter η initially decreases from 1.0 (380 K) to 0.33 (460 K), and then it increases again up to 0.56 (575 K). The quadrupole coupling constant increases from 9.4 to 12.2 kHz in the same temperature range (see Fig. 2).

A new weak triplet (*E*) appears in the ${}^7\text{Li}$ NMR spectrum at the temperature corresponding to the minimum of the $\eta(T)$ dependence. The intensity of the *E* triplet increases with increasing temperature and reaches about 5% of the total intensity of the spectrum at 575 K. The

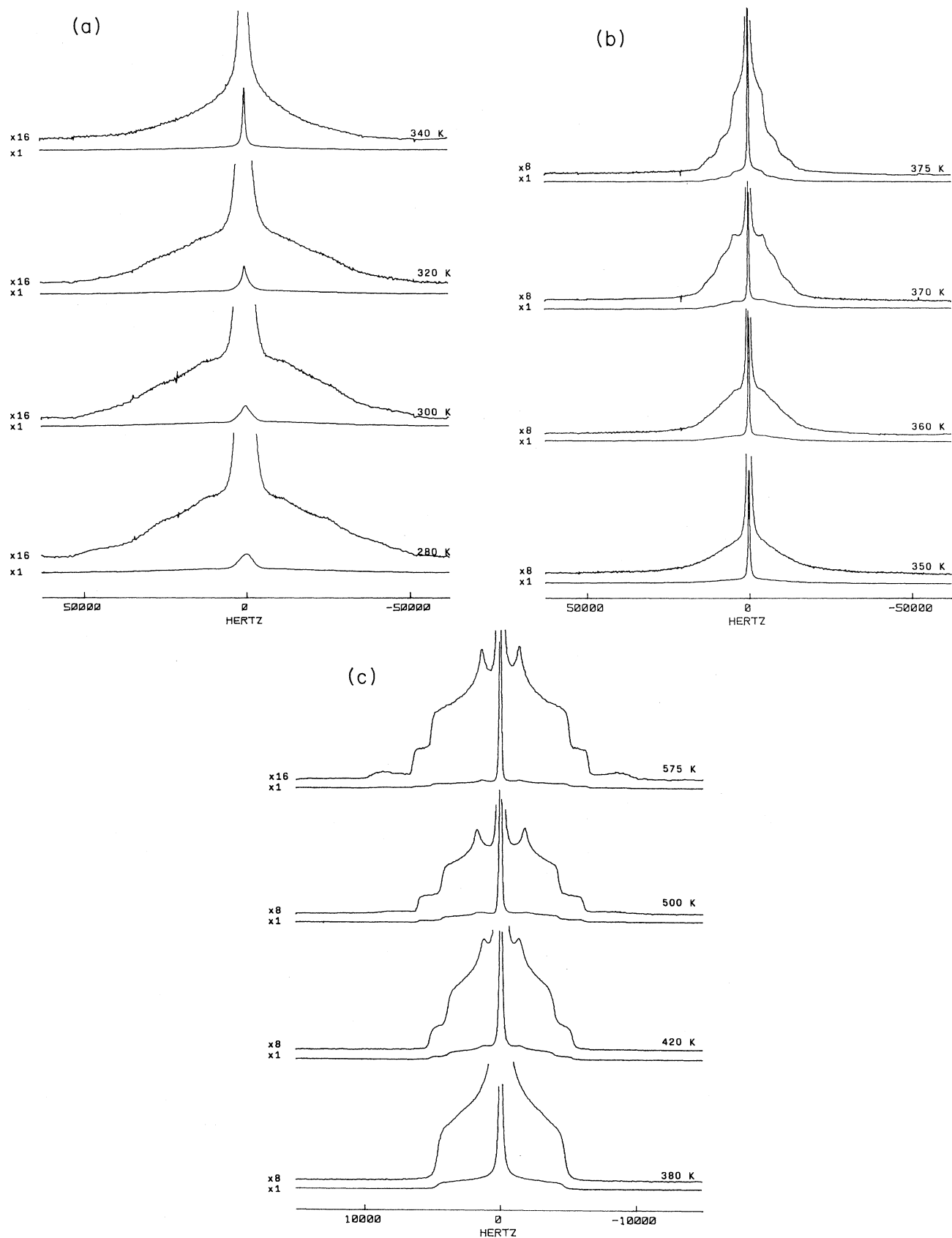


FIG. 1. ${}^7\text{Li}$ FT NMR spectrum of monoclinic $\text{Li}_3\text{In}_2(\text{PO}_4)_3$ at different temperatures.

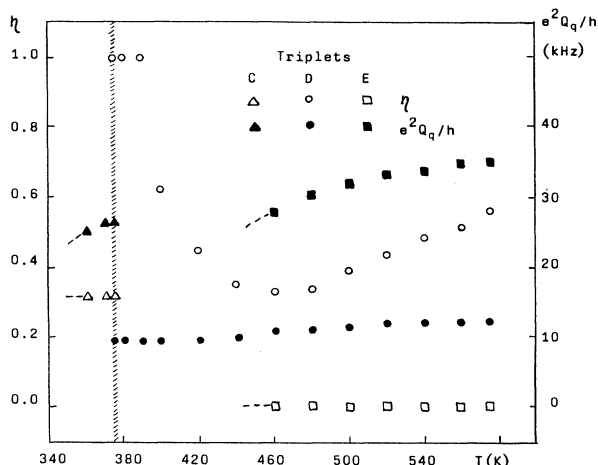


FIG. 2. Temperature dependences of the e^2Qq/h and η parameters of the C , D , and E quadrupole triplets in the ${}^7\text{Li}$ spectrum of monoclinic $\text{Li}_3\text{In}_2(\text{PO}_4)_3$. The temperature range corresponding to the phase transition ($T_c \approx 375$ K) is shaded.

quadrupole coupling constant of the E triplet progressively increases from ≈ 28 kHz (460 K) to 34.8 kHz (575 K), whereas the asymmetry parameter η does not depend on the temperature and remains about zero.

It should be noted that all the observed transformations of the ${}^7\text{Li}$ NMR spectrum take place without a noticeable hysteresis under temperature cycling.

B. Intensity of the ${}^7\text{Li}$ NMR spectra

Figure 3 shows the temperature dependences of the reciprocal integral intensity (I^{-1}) of the ${}^7\text{Li}$ NMR spectra of monoclinic $\text{Li}_3\text{In}_2(\text{PO}_4)_3$, $\text{Li}_3\text{Sc}_2(\text{PO}_4)_3$, and rhombohedral $\text{Li}_3\text{In}_2(\text{PO}_4)_3$. The value of I^{-1} is set equal to 1.0 at 300 K.

Because the I value is directly proportional to the nuclear magnetization of a sample, $M_0 = \chi_0 H_0$ (where χ_0 is the static nuclear magnetic susceptibility and H_0 is the external magnetic field), the dependences of $I^{-1}(T)$ shown in Fig. 3 follow the temperature changes of χ_0 :

$$\chi_0^{-1} = 3kT/N\gamma^2(H/2\pi)^2 S(S+1), \quad (1)$$

where k is the Boltzmann constant, N is the number of ${}^7\text{Li}$ nuclei per unit volume, γ is the gyromagnetic ratio of the ${}^7\text{Li}$ nucleus, S is the spin of ${}^7\text{Li}$ ($\frac{3}{2}$), and h is the Planck constant.

As can be seen from Fig. 3, the obtained dependences pointed to an anomalous temperature behavior of χ_0 . The $\chi_0^{-1}(T)$ curve is a straight line passing through the origin according to the Curie law. However, in Fig. 3 the Curie law is satisfied only within the temperature ranges ≤ 310 and ≥ 380 K for monoclinic $\text{Li}_3\text{In}_2(\text{PO}_4)_3$, $T \leq 320$ and ≥ 460 K for rhombohedral $\text{Li}_3\text{In}_2(\text{PO}_4)_3$, and $T \leq 330$ and ≥ 540 K for monoclinic $\text{Li}_3\text{Sc}_2(\text{PO}_4)_3$. It should be stressed that the slopes of the experimental $\chi_0^{-1}(T)$ curves in Fig. 3 are less in the high-temperature range

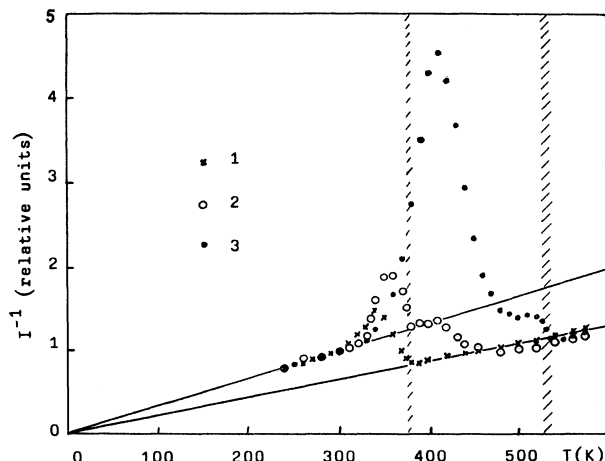


FIG. 3. Temperature dependences of the reciprocal integral intensity I^{-1} of the ${}^7\text{Li}$ spectra of the monoclinic (1) and rhombohedral (2) $\text{Li}_3\text{In}_2(\text{PO}_4)_3$ and monoclinic $\text{Li}_3\text{Sc}_2(\text{PO}_4)_3$ (3). The temperature ranges corresponding to the phase transitions are shaded.

than in the low-temperature range by a factor of 1.6.

To be certain that the intensity of the observed ${}^7\text{Li}$ NMR spectra is caused by contributions of all the lithium nuclei in the samples, we have compared the spectral intensities of these compounds with the intensity of the ${}^7\text{Li}$ NMR spectrum of a sample exhibiting no anomalies of χ_0^{-1} in the entire temperature range. Li_2HfO_3 was used as the sample. The ${}^7\text{Li}$ NMR spectrum of Li_2HfO_3 has a well-resolved quadrupole structure at $T \leq 300$ K, and the $I^{-1}(T)$ dependence for this compound strictly obeys the Curie law in the temperature range 240–575 K.⁶

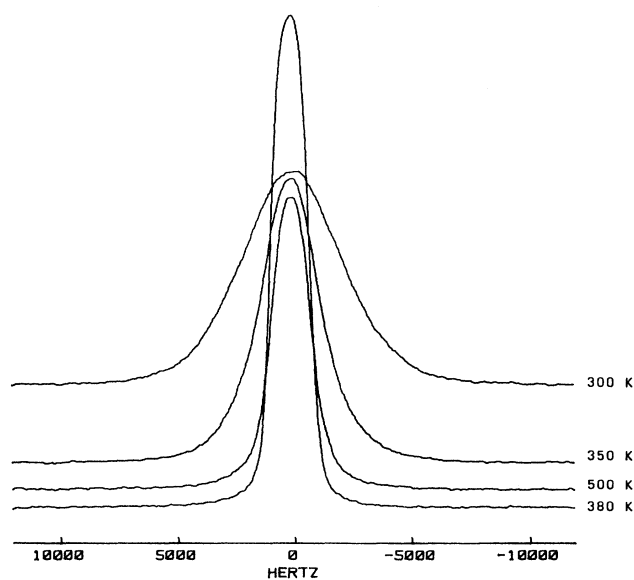


FIG. 4. ${}^{31}\text{P}$ FT NMR spectrum of monoclinic $\text{Li}_3\text{In}_2(\text{PO}_4)_3$ at different temperatures.

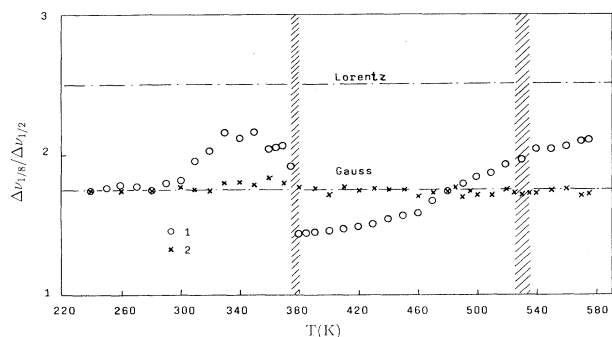


FIG. 5. Temperature dependences of the ratio $\Delta v_{1/8}/FWHH$ for the ^{31}P line in monoclinic $\text{Li}_3\text{In}_2(\text{PO}_4)_3$ (1) and $\text{Li}_3\text{Sc}_2(\text{PO}_4)_3$ (2). The temperature ranges corresponding to the phase transitions are shaded.

Thus it was established that the observed ^7Li NMR spectra of the studied phosphates result from contributions from all the lithium nuclei in their crystal structure.

C. ^{31}P NMR spectra

Figure 4 shows the ^{31}P FT NMR spectrum of monoclinic $\text{Li}_3\text{In}_2(\text{PO}_4)_3$ at different temperatures. This spectrum consists of a single line in the entire temperature range as well as the ^{31}P NMR spectra of rhombohedral $\text{Li}_3\text{In}_2(\text{PO}_4)_3$ and monoclinic $\text{Li}_3\text{Sc}_2(\text{PO}_4)_3$.^{3,4}

However, changes of the ^{31}P line shape are observed in monoclinic $\text{Li}_3\text{In}_2(\text{PO}_4)_3$ with increasing temperature, in contrast to the lithium phosphates studied in Refs. 3 and 4.

To classify the observed ^{31}P line shape either as Gaussian or Lorentzian, we have used ratio of $\Delta v_{1/8}/FWHH$, where $\Delta v_{1/8}$ is the linewidth at $\frac{1}{8}$ height and FWHH is full width at half height of the line. The values of the ratio have to be equal either to 1.75 or 2.5 for the canonical Gaussian or Lorentzian line shape, respectively.

Figure 5 shows the temperature dependences of the ratio for the ^{31}P NMR line in monoclinic $\text{Li}_3\text{In}_2(\text{PO}_4)_3$ and

$\text{Li}_3\text{Sc}_2(\text{PO}_4)_3$. As can be seen from Fig. 5, the ^{31}P line shape is Gaussian and does not depend on temperature in $\text{Li}_3\text{Sc}_2(\text{PO}_4)_3$. In monoclinic $\text{Li}_3\text{In}_2(\text{PO}_4)_3$ the Gaussian line shape is observed only below 310 K. With increasing temperature from 310 to 370 K, the Gaussian gradually tends to the Lorentzian. However, the $\Delta v_{1/8}/FWHH$ ratio discontinuously decreases to a value significantly less than 1.75 in the temperature range 375–380 K. Under the following temperature increase (> 380 K, the ^{31}P line shape again gradually tends to the Lorentzian “passing” through the Gaussian.

It should be noted that the $I^{-1}(T)$ dependences of the ^{31}P FT NMR spectra for both $\text{Li}_3\text{In}_2(\text{PO}_4)_3$ and $\text{Li}_3\text{Sc}_2(\text{PO}_4)_3$ strictly follow the Curie law in the entire temperature range.

D. ^7Li and ^{31}P spin-lattice relaxation rates

Figure 6 shows the temperature dependences of the spin-lattice relaxation rates $1/T_1$ for ^7Li and ^{31}P in monoclinic $\text{Li}_3\text{In}_2(\text{PO}_4)_3$. The temperature dependences of $1/T_1$ for ^7Li and ^{31}P in monoclinic $\text{Li}_3\text{Sc}_2(\text{PO}_4)_3$ are shown in this figure for comparison.

The recovery of the longitudinal magnetization for both ^7Li and ^{31}P is well described by a single exponent in the entire temperature range.

The values of $1/T_1$ for ^7Li and ^{31}P in $\text{Li}_3\text{In}_2(\text{PO}_4)_3$ exceed the corresponding values of $1/T_1$ in $\text{Li}_3\text{Sc}_2(\text{PO}_4)_3$ approximately in order of magnitude at $T \leq 300$ K. In this temperature range, the ^7Li and ^{31}P spin-lattice relaxation rates depend only weakly on temperature and can be controlled by spin diffusion to the paramagnetic impurities as has been suggested elsewhere.⁴ The almost equal values of $1/T_1$ for ^{31}P obtained below 300 K in both monoclinic and rhombohedral $\text{Li}_3\text{In}_2(\text{PO}_4)_3$ can be considered as a confirmation of this suggestion because of the same impurity level in the initial reagents used for the synthesis of the compounds.

The relaxation rates for ^7Li and ^{31}P in monoclinic $\text{Li}_3\text{In}_2(\text{PO}_4)_3$ progressively increase in the temperature range 310–375 K. They are believed to be controlled by

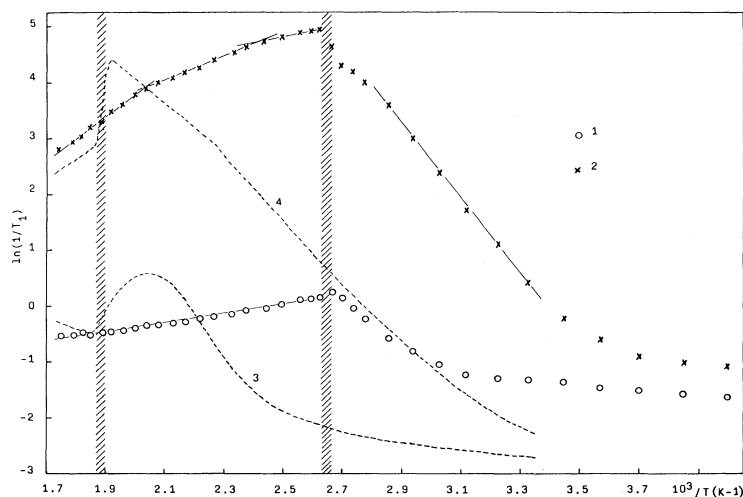


FIG. 6. Experimental temperature dependences of the spin-lattice relaxation rates (s^{-1}) for ^7Li (2,4) and ^{31}P (1,3) in monoclinic $\text{Li}_3\text{In}_2(\text{PO}_4)_3$ (1,2) and $\text{Li}_3\text{Sc}_2(\text{PO}_4)_3$ (3,4). [Data on monoclinic $\text{Li}_3\text{Sc}_2(\text{PO}_4)_3$ were taken from Ref. 4.]

the motion of the lithium ions. However, solid data on the activation energy of this motion (E_a) can be obtained in this temperature range only from the slope of the temperature dependence $\ln(1/T_1)$ for ${}^7\text{Li}$. This value of E_a is about 56 kJ/mol.

The temperature dependences of the spin-lattice relaxation rates reach the maxima at 375 and 380 K for ${}^{31}\text{P}$ and ${}^7\text{Li}$, respectively. One further extremum is visible in the $1/T_1$ curve for ${}^7\text{Li}$ in the interval 365–370 K (see Fig. 6). With the following temperature increase, the $1/T_1$ value for ${}^{31}\text{P}$ in monoclinic $\text{Li}_3\text{In}_2(\text{PO}_4)_3$ gradually decreases, approximately following a linear law in the range 385–575 K. The activation energy calculated from the slope of this line is about 7 kJ/mol.

The $1/T_1$ value for ${}^7\text{Li}$ rapidly decreases with respect to $1/T_1$ for ${}^{31}\text{P}$ in the same temperature range. Besides, the dependence does not obey the Arrhenius law (at least three exponents are necessary to describe the temperature behavior of the ${}^7\text{Li}$ spin-lattice relaxation rate above 385 K.

III. DISCUSSION

A. ${}^7\text{Li}$ NMR spectra

There is scarcely any difference between the ${}^7\text{Li}$ FT NMR spectra of monoclinic $\text{Li}_3\text{In}_2(\text{PO}_4)_3$, rhombohedral $\text{Li}_3\text{In}_2(\text{PO}_4)_3$,³ and monoclinic $\text{Li}_3\text{Sc}_2(\text{PO}_4)_3$ (Ref. 4) at the temperatures below 300 K. These spectra might be classified as quadrupole triplets for a spin of $\frac{3}{2}$. In such a case, the satellite part *A* is not resolved due to a wide distribution of the components of the electrical field gradient (EFG) by magnitude and orientation. The central part *B* is broadened only due to dipole-dipole interactions of the ${}^7\text{Li}$ nuclei with adjacent magnetic nuclei.

However, the following experimental data are in conflict with this suggestion.

First of all, the experimental ratio of the intensities of the *A* to *B* components is about 4:1. For the canonical quadrupole triplet for spins of $\frac{3}{2}$, it should be equal to 3:2. On the other hand, the attribution of the experimental ${}^7\text{Li}$ NMR spectrum as an unresolved quadrupole triplet contradicts the disappearance of the broad component *A* with increasing temperature. Besides, in the case of the unresolved quadrupole triplet the satellite part *A* has to decrease in its extension and increase in its amplitude, keeping the same integral intensity of the spectrum.

Taking this into account, one attributes the ${}^7\text{Li}$ NMR spectra observed below 300 K as a superposition of two dipolarly broaden singlets *A* and *B* with the same value of the chemical shift. Then, using the values of the extension of both *A* and *B* singlets, one can estimate the effective distance between the spins composing an isolated pair within the Pake model.⁷ The distance was found to be approximately the sum of the radii of two lithium ions (≈ 1.3 Å) for the *A* singlet and about 2.5 Å for the *B* singlet. It allows one to consider the *A* component as resulting from contributions of “contact” pairs of lithium ions, whereas the *B* component from contributions of lithium ions situated at the distances determined with diffraction techniques for low-temperature modifications of the crystals.^{1,5}

A distinguishing feature of the studied superionics with the point of view of NMR is a well-resolved quadrupole structure of the ${}^7\text{Li}$ NMR spectra in the high-temperature range where $\tau_c\omega_Q \ll 1$. Here τ_c is the correlation time for the motion of lithium ions and ω_Q is the quadrupole frequency. As a rule, the quadrupole structure of NMR spectra in solids is not observed due to its collapsing to a singlet line when the inequality $\tau_c\omega_Q \ll 1$ is obeyed. Therefore the observation of a well-resolved quadrupole structure of the ${}^7\text{Li}$ NMR spectra under the $\tau_c\omega_Q \ll 1$ condition indicates that τ_c is divorced from dynamic processes, resulting in a variation of magnitude and orientation of the corresponding components of the EFG tensor.

To account for the obtained data, a model of a “frozen” EFG was suggested.⁴ According to this model, the lithium ions move at a rate $1/\tau_c$ over the equivalent sites. This equivalence means that the components of the EFG tensor are the same in all these sites and do not depend on time and temperature (i.e., “frozen”). In such a case, a quadrupole structure of the ${}^7\text{Li}$ NMR spectra will be observed even if $\tau_c\omega_Q \ll 1$. The motion of the lithium ions will result in a narrowing of the NMR line only due to the averaging of the ${}^7\text{Li}$ dipole-dipole interactions with the adjacent magnetic nuclei within the approach.

B. Static magnetic susceptibility of lithium nuclei

As was shown in Sec. II B, the relative values of χ_0 in the high-temperature range are more than the χ_0 values in the low-temperature range by a factor of 1.6. Assuming that the static magnetic susceptibility of the lithium subsystem is due to N ${}^7\text{Li}$ nuclei with spin S ($\frac{3}{2}$) at 300 K, we will obtain that the value of χ_0 corresponds to $N/2$ ${}^7\text{Li}$ nuclei with spin S' (3) above 380 K [$\text{Li}_3\text{In}_2(\text{PO}_4)_3$] or 540 K [$\text{Li}_3\text{Sc}_2(\text{PO}_4)_3$]. In other words, the nuclear magnetism of the lithium subsystems of the crystals is due to ortho pairs ($S=3$) (Ref. 4) in the high-temperature region. The ortho pairs undergo an ortho-to-para transition as the temperature decreases. Taking into account that $S=0$ for the para state, one can understand the observed decrease of χ_0 . At temperatures below the minima in the $\chi_0^{-1}(T)$ curve, the spin-spin correlations in the lithium subsystem disappear. So at $T \leq 300$ K the χ_0 value is due to individual contributions of the lithium ions.

We recognize that the “para-ortho” model is vulnerable for many reasons. However, it allows one to obtain quantitative agreement between the χ_0 values in the low- and high-temperature regions.

When the $I^{-1}(T)$ dependences are compared with the temperature behavior of the ${}^7\text{Li}$ NMR spectra in all of the phosphates studied, it is apparent that χ_0 decreases simultaneously with the disappearance of the broad component *A* and increases with appearance of the *C* quadrupole triplet.

It should be mentioned that temperature behavior of intensity of the ${}^7\text{Li}$ NMR spectrum (and correspondingly χ_0) strictly follows the Curie law in lithium containing compounds which exhibit no superionic properties [for example, Li_2MO_3 with $M = \text{Ti, Zr, Hf}$ (Ref. 6)]. It allows

one to suggest that the anomalous temperature behavior of the magnetic susceptibility of lithium in the studied superionics is associated with an increase of the mobility of lithium ions.

C. ^{31}P NMR spectra

The experimental ^{31}P NMR spectra obtained for monoclinic $\text{Li}_3\text{In}_2(\text{PO}_4)_3$ were analyzed with LINESIM software. The results of the simulation show that the experimental ^{31}P NMR spectrum can be fitted with a single Gaussian line at $T < 310$ K only. Above that temperature two lines are required to fit the spectrum.

The ^{31}P spectrum can be simulated as a superposition of two lines of the same chemical shift but different in width in the temperature ranges 310–370 and ≥ 380 K. One of these lines (narrow) has the Gaussian line shape, while another line (broad) has the Lorentzian line shape. Herewith the relative intensities of these lines depend on temperature. In the range 375–380 K, the experimental data can be fitted using two Gaussians of equal intensity but different values of the chemical shift (≈ 7 ppm).

If it is granted that the fitting of the ^{31}P NMR spectra with two lines is caused by a real physical process in the samples (for example, the existence of magnetically non-equivalent positions of the phosphorus nuclei, anisotropy of the chemical shift, and so on), these lines have to manifest themselves as more pronounced in the ^{31}P line shape at higher frequencies. The ^{31}P FT NMR spectra of monoclinic $\text{Li}_3\text{In}_2(\text{PO}_4)_3$ were recorded at 121.45 MHz to check this suggestion. However, the observed temperature changes of the ^{31}P line shape do not vary with respect to the frequency 36.44 MHz. Thus the fitting of the experimental ^{31}P spectra with two lines is a pure mathematical procedure which has no real physical basis.

The unusual temperature behavior of the ^{31}P NMR line shape above 310 K does not allow one to obtain solid data on the second moment of the line and calculate the effective distances between the dipole-dipole interacting nuclei (P-Li, P-P, and P-In).

D. ^7Li and ^{31}P spin-lattice relaxation

The temperature dependences of the ^7Li and ^{31}P spin-lattice relaxation rates can be ascribed within modern approaches to nuclear magnetic relaxation at $T \leq 370$ K for monoclinic $\text{Li}_3\text{In}_2(\text{PO}_4)_3$ and $T \leq 520$ K for monoclinic $\text{Li}_3\text{Sc}_2(\text{PO}_4)_3$. For example, the temperature dependences of $1/T_1$ for ^7Li and ^{31}P may be classified as caused by spin diffusion at $T < 300$ K and a motion of lithium ions with correlation time τ_c in the ranges 310–370 K [monoclinic $\text{Li}_3\text{In}_2(\text{PO}_4)_3$] and 340–520 K [monoclinic $\text{Li}_3\text{Sc}_2(\text{PO}_4)_3$].⁴ The latter allows one to calculate the length of the dipole-dipole relaxation vector within the Blombergen-Purcell-Pound model.⁸ Herewith the τ_c value can be evaluated using a procedure suggested elsewhere.⁴

The calculated length of the vector of dipolar relaxation (or in other words the effective internuclear distance controlling the ^7Li spin-lattice relaxation rate) is approximately the sum of the radii of two lithium ions. This re-

sult again confirms the presence of the “contact” pairs of ^7Li ions in the crystal structure of the phosphates. It should be noted that the ^7Li spin-lattice relaxation rate is explicitly unaffected by the quadrupole interaction. It follows from the absence of EFG fluctuations in the lithium sites, which is proved by the pronounced quadrupole structure of the ^7Li NMR spectra at $\tau_c \omega_Q \ll 1$.

The ^{31}P spin-lattice relaxation rate in monoclinic $\text{Li}_3\text{In}_2(\text{PO}_4)_3$ is controlled by the ^{31}P - ^7Li dipole-dipole interaction in the range 310–370 K. The corresponding correlation time is identical to τ_c for the motion of lithium ions. The length of the vector of the dipolar relaxation approximately equals the P-Li distance obtained with structural analysis of the compound (≈ 2.8 Å). Contributions of the ^7Li - ^6Li , ^7Li - ^{17}O , ^{31}P - ^6Li , and ^{31}P - ^{17}O dipole-dipole interactions to the observed spin-lattice relaxation rates are insignificant because of a low content of the ^6Li and ^{17}O isotopes in the samples.

Approaches different from the canonical models are necessary to account for the temperature dependences of $1/T_1$ for ^7Li and ^{31}P in monoclinic $\text{Li}_3\text{In}_2(\text{PO}_4)_3$ at $T > 380$ K and monoclinic $\text{Li}_3\text{Sc}_2(\text{PO}_4)_3$ above 540 K.

E. Comparison of the NMR data with the results of conductivity measurements, structural analysis, and differential scanning calorimetry

A single distinct anomaly is observed in the differential scanning calorimetry (DSC) curve each of the compounds in the temperature range 300–600 K (see Fig. 7). The corresponding C_p maximum lies at 368 K [monoclinic $\text{Li}_3\text{In}_2(\text{PO}_4)_3$], 382 K [rhombohedral $\text{Li}_3\text{In}_2(\text{PO}_4)_3$ (Ref. 2)], and 535 K [monoclinic $\text{Li}_3\text{Sc}_2(\text{PO}_4)_3$ (Ref. 4)]. As was earlier suggested,^{2–4} the anomaly is caused by structural phase transitions of the first order. The above-mentioned values of T_c agree well with the temperatures wherein changes in the NMR spectra and temperature dependences of $1/T_1$ for ^7Li and ^{31}P are observed. So it can be concluded that the changes that occur in the vicinity of T_c are associated with the structural phase transitions in

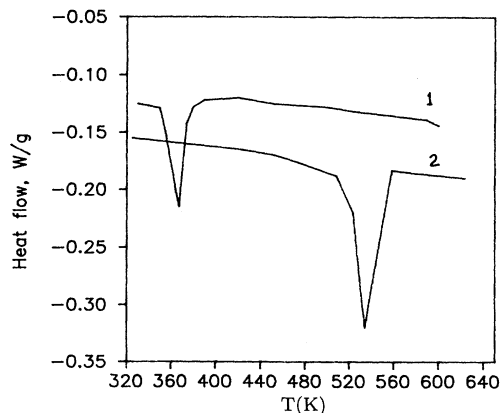


FIG. 7. DSC curves for monoclinic $\text{Li}_3\text{In}_2(\text{PO}_4)_3$ (1) and $\text{Li}_3\text{Sc}_2(\text{PO}_4)_3$ (2). [Data on monoclinic $\text{Li}_3\text{Sc}_2(\text{PO}_4)_3$ were taken from Ref. 4.]

the compounds.

The temperature dependences of the ionic conductivity for the phosphates also point to structural phase transitions at the corresponding T_c (see Fig. 8). However, the behavior of $\sigma(T)$ near T_c is different in character for $\text{Li}_3\text{In}_2(\text{PO}_4)_3$ and $\text{Li}_3\text{Sc}_2(\text{PO}_4)_3$. As concerns NMR, the changes of the corresponding ${}^7\text{Li}$ spectra are practically identical. These changes can be summarized as follows.

(i) Below the phase transition point, the broad component A disappears; the static magnetic susceptibility χ_0 initially decreases, then increases, and becomes greater than the χ_0 value at 300 K; the C triplet appears with a well-resolved quadrupole structure.

(ii) In the vicinity of T_c , the second quadrupole triplet D appears by an "abrupt jump"; the triplet exists simultaneously with the C triplet in a narrow temperature interval ≤ 5 K [$\text{Li}_3\text{In}_2(\text{PO}_4)_3$] and ≤ 15 K [$\text{Li}_3\text{Sc}_2(\text{PO}_4)_3$]; the parameters of these triplets are significantly different.

(iii) Above the superionic phase-transition point, the D triplet completely substitutes the C triplet; an increase of χ_0 is completed; it becomes more than χ_0 at 300 K by a factor of 1.6.

The observed changes of the ${}^7\text{Li}$ NMR spectra from the two singlets to a one quadrupole triplet seem to indicate the existence of several different lithium positions sequentially occupied with increasing temperature. The anomalous behavior of χ_0 is completed above T_c . Hence it follows that its changes seem to connect with transitions to the superionic state. The latter means that a relation has to exist between the changes of the static magnetic susceptibility of the lithium nuclei subsystem and the dynamics of the lithium ions.

There are cases when the intensity of the NMR spectrum either only decreases or increases on heating of a sample.⁹⁻¹² In the first case, it is suggested that some quantity of the nuclei is in positions characterized by very long relaxation times. As a result, these nuclei become "invisible." In the second case, in contrast, the relaxation time of the "invisible" nuclei decreases with increasing temperature. The situation when the intensity of the NMR spectrum with increasing temperature ini-

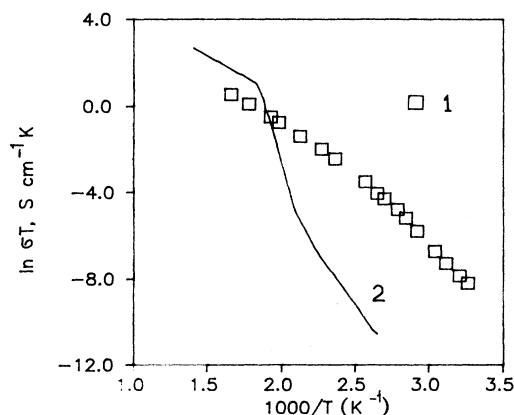


FIG. 8. Temperature dependences of the ionic conductivity of monoclinic $\text{Li}_3\text{In}_2(\text{PO}_4)_3$ (1) and $\text{Li}_3\text{Sc}_2(\text{PO}_4)_3$ (2). [Data on monoclinic $\text{Li}_3\text{Sc}_2(\text{PO}_4)_3$ were taken from Ref. 4.]

tially decreases, then increases, and exceeds the low-temperature value is observed in this work. It should be stressed that we suggest another mechanism of decrease of the NMR spectra intensity than "trapping" of the nuclei into sites with long T_1 . It follows in particular from the unsuccessful attempts to reveal the "invisible" nuclei of ${}^7\text{Li}$ in the studied samples by an increase of the delay time between the pulse sequence and accumulation quantity of the NMR signal (up to 10^4 s).

In accordance with the obtained NMR data, there are two types of positions of the lithium ions in the vicinity of the superionic phase transition. Above the phase-transition point, only one type of position is observed in both monoclinic phosphates. This seems contrary to the diffraction data, which point to the existence of several types of lithium sites in the entire temperature range.¹³

Parameters of the ${}^7\text{Li}$ quadrupole spectra for the monoclinic phosphates below and above the superionic transformation temperature are listed in Table I. As can be seen from Table I, the parameters vary in a similar way. The relative changes of the parameters are very close. However, a comparison of the absolute values of the parameters indicates a different symmetry of the lithium sites below and above T_c . Indeed, the quadrupole constant corresponding to the D triplet is less than the constant corresponding to the C triplet. It indicates a decrease of the value of the main component of the EFG tensor on ${}^7\text{Li}$ nuclei. This may be due to either an increase in the length of the Li-O bond or to the fact that this bond slackens under transition to the superionic state.

The ${}^7\text{Li}$ and ${}^{31}\text{P}$ NMR data on monoclinic $\text{Li}_3\text{In}_2(\text{PO}_4)_3$ bring out structural and dynamic features of the superionic transition which were not detected with the diffraction and dielectrical studies. First of all, this is the temperature dependence of the asymmetry parameter η of the D triplet (see Sec. II A). As can be seen from Fig. 1, the geometry of the EFG is initially "two-dimensional" ($V_{zz} = V_{xx} \neq 0$, $V_{yy} = 0$), corresponding to $\eta = 1.0$ (near T_c). Then the geometry transforms to a "three-dimensional" one ($V_{zz} \neq V_{xx} \neq V_{yy}$), corresponding to $\eta = 0.33$. This "three-dimensional" geometry again tends to the "two-dimensional" one as the temperature increases in the range 460–575 K. This is evidenced by increasing the value of η from 0.33 to 0.56. It is noteworthy that the process is accompanied by the appearance of the E quadrupole triplet in the ${}^7\text{Li}$ spectrum.

This triplet has parameters identical to the parameters of the quadrupole triplet in the ${}^7\text{Li}$ NMR spectrum in

TABLE I. Parameters of the quadrupole triplets in the ${}^7\text{Li}$ NMR spectra of monoclinic $\text{Li}_3\text{In}_2(\text{PO}_4)_3$ and $\text{Li}_3\text{Sc}_2(\text{PO}_4)_3$ below and above the superionic phase transition.

Compound	Below the superionic phase transition		Above the superionic phase transition	
	e^2qQ/h (kHz)	η	e^2qQ/h (kHz)	η
$\text{Li}_3\text{In}_2(\text{PO}_4)_3$	26.4	0.31	12.2	0.56
$\text{Li}_3\text{Sc}_2(\text{PO}_4)_3$	45.0	0.23	22.3	0.43

rhombohedral $\text{Li}_3\text{In}_2(\text{PO}_4)_3$.³ However, the intensity of this triplet is about $\frac{2}{3}$ of the total intensity of the ^7Li spectrum in the latter compound. The appearance of the E triplet in the ^7Li spectrum of monoclinic $\text{Li}_3\text{In}_2(\text{PO}_4)_3$ can be caused by the onset of a martensite-type phase transition to the rhombohedral phase. This suggestion is supported by the data,² indicating the appearance of a rhombohedral phase under annealing of monoclinic $\text{Li}_3\text{In}_2(\text{PO}_4)_3$ at mediative temperatures (≈ 800 K).

As can be seen from Figs. 6 and 8, the $1/T_1$ rates for ^7Li (and ^{31}P) are the same in monoclinic $\text{Li}_3\text{In}_2(\text{PO}_4)_3$ and $\text{Li}_3\text{Sc}_2(\text{PO}_4)_3$ at ≈ 540 K. This temperature also corresponds to the equivalence of the values of σ of the compounds. This result allows us to suggest that the same process is responsible for the temperature behavior of both the spin-lattice relaxation rate and ionic conductivity. It is natural to assume that the process is the motion of the lithium ions. Indeed, the diffusion coefficient (D) for the lithium ions in $\text{Li}_3\text{Sc}_2(\text{PO}_4)_3$ calculated from the ionic conductivity data using the Nernst-Einstein relation (5×10^{-12} m/s²) is approximately equal to the value of D obtained as $D = \langle R^2 \rangle / 6\tau_c$ from the NMR data [$\langle R^2 \rangle$ is the mean-square P-Li distance (2.8 Å), and τ_c is obtained from the maximum of the temperature dependence of $1/T_1$ for ^{31}P (Ref. 4)].

The difference between the values of the activation energy of ion transport obtained from the temperature dependences of $1/T_1$ (for ^7Li) and σ is insignificant in the monoclinic phosphates far below T_c . Above T_c the temperature dependence of the spin-lattice relaxation rate in monoclinic $\text{Li}_3\text{In}_2(\text{PO}_4)_3$ exhibits a non-Arrhenius behavior (see Sec. IID). The behavior can be caused by the above-mentioned phase transition to the rhombohedral modification of $\text{Li}_3\text{In}_2(\text{PO}_4)_3$. The nonexponentiality of the $(1/T_1)$ (T) dependence does not allow one to calculate the activation energy of the lithium motion with studies of the ^7Li relaxation. However, suggesting that the lithium motion controls spin-lattice relaxation both ^7Li and ^{31}P , one can obtain the corresponding value of E_a from the temperature dependence of $1/T_1$ for ^{31}P .

The value of E_a calculated in this way is surprisingly lower than the value of E_a obtained from the $\sigma(T)$ dependence for $\text{Li}_3\text{In}_2(\text{PO}_4)_3$ (7 and 34 kJ/mol, respectively).

This leads to the interesting conclusion on the high-frequency dispersion of σ below and above the T_c point. In accordance with the Funke model for jump relaxation in solids,¹⁴ the dispersion ($\propto 1 - E_a^{\text{NMR}}/E_a^\sigma$) has to increase in the superionic phase (below T_c the corresponding activation energies are approximately equal).

It is worth noting that the character of the temperature dependence of ionic conductivity of monoclinic $\text{Li}_3\text{In}_2(\text{PO}_4)_3$ above T_c allows one to use the Vogel-Fulcher-Tammann-Hesse (VFTH) approach¹⁵⁻¹⁷ for its description. Scaling the data within the VFTH model, the E_a^{VFTH} value obtained is about 18 kJ/mol. This is significantly lower than the E_a value calculated above within the Arrhenius approach. It is not so easy to decide which value of E_a corresponds to the real activation energy of the ion charge transfer in the compound. A thorough analysis of this problem is out of the scope of this paper.

IV. CONCLUSIONS

Quantitative and qualitative data have been obtained on the structural features, interionic interactions, and dynamics of both mobile and immobile subsystems in superionic $\text{Li}_3\text{In}_2(\text{PO}_4)_3$ and $\text{Li}_3\text{Sc}_2(\text{PO}_4)_3$. However, these results raise many new problems. This is particularly true for anomalous changes of the intensity of the ^7Li NMR spectrum. Besides, the observed changes of the ^{31}P NMR line shape in monoclinic $\text{Li}_3\text{In}_2(\text{PO}_4)_3$ are also rather surprising. The nature of these phenomena is not clear yet, and they cannot be accounted for within existing theoretical approaches to nuclear magnetism. New ideas also are necessary for the description of the temperature behavior of the ^{31}P spin-lattice relaxation rates of the compounds in the superionic state. The observed unusual phenomena seem to be associated with still poorly understood properties of the superionic solids.

ACKNOWLEDGMENTS

The authors wish to thank Dr. A. A. Samoylenko (Bruker Moscow Service Center) for providing the LINESIM computer-simulation software and for the use of the Bruker MSL-300 spectrometer.

*Present address: Institut für Physikalische Chemie Westfälische-Wilhelms Universität, Schlossplatz 4, Münster 48149 Germany.

¹A. B. Bykov *et al.*, *Solid State Ion.* **38**, 31 (1990).

²Yu. K. Naganovsky and S. E. Sigaryov, *Solid State Ion.* **50**, 1 (1992).

³I. S. Pronin, S. E. Sigaryov, and A. A. Vashman, *Solid State Ion.* **38**, 9 (1990).

⁴A. A. Vashman, I. S. Pronin, and S. E. Sigaryov, *Solid State Ion.* **58**, 201 (1992).

⁵D. Tran Qui and S. Hamdoune, *Acta Crystallogr. C* **43**, 397 (1987).

⁶I. S. Pronin *et al.*, *Zh. Neorg. Khim.* **35**, 1827 (1990).

⁷G. E. Pake, *J. Chem. Phys.* **16**, 327 (1948).

⁸N. Blombergen, E. M. Purcell, and R. V. Pound, *Phys. Rev.* **73**, 679 (1948).

⁹J. W. Akitt, *J. Chem. Soc. Dalton Trans.* **1**, 42 (1973).

¹⁰R. E. Walstedt, R. Dupree, J. P. Remeika, and A. Rodriguez, *Phys. Rev. B* **15**, 3442 (1977).

¹¹J. L. Bjorkstam, M. Villa, and G. C. Farrington, *Solid State Ion.* **5**, 153 (1981).

¹²S. P. Gabuda, R. N. Pletnyov, and M. A. Fedotov, in *Nuclear Magnetic Resonance in Inorganic Chemistry*, edited by V. A. Gubanov (Nauka, Moscow, 1988), p. 100 (in Russian).

¹³S. E. Sigaryov, E. A. Genkina, and B. A. Maximov, *Solid State Ion.* **37**, 261 (1990).

¹⁴K. Funke, in *Solid State Ionics II*, edited by G.-A. Nazri, R. A. Huggins, and F. D. Shriver (Material Research Society, Pittsburgh, 1989), p. 43.

¹⁵H. Vogel, *Phys. Z.* **22**, 645 (1921).

¹⁶G. S. Fulcher, *J. Am. Ceram. Soc.* **8**, 339 (1925).

¹⁷G. Tammann and G. Hesse, *Z. Anorg. Allg. Chem.* **156**, 245 (1926).